5-16-2022

Thermal Energy Storage and Cooling Capability of Composite Field's Metal and Paraffin Phase Changing Material (May 2022)

Rahi Miraftab-Salo
Washington University in St. Louis

Thermal Energy Storage and Cooling Capability of Composite Field's Metal and Paraffin Phase Changing Material (May 2022)

RAHI MIRAFTAB-SALO[1], BIDISHA OHJA[2], KIDUS GUYE [3] AND DAMENA. AGONAFER.[4],

[1]Washington University in St. Louis, MO, 63105, USA (e-mail: rahi.m@wustl.edu)
[2]Washington University in St. Louis, MO, 63105, USA (e-mail: b.ojha@wustl.edu)
[3]Washington University in St. Louis, MO, 63105, USA (e-mail: g.kidus@wustl.edu)
[3]Washington University in St. Louis, MO, 63105, USA (e-mail: agonafer@wustl.edu)

ABSTRACT Phase change materials (PCMs) have the ability to increase the efficiency of energy-intensive applications, through absorbing a significant amount of latent heat during phase change. More specifically, composite PCM's, consisting of an organic PCMs (e.g., paraffin) and inorganic (e.g., metallic alloys and salt hydrates) material, provide a superior balance of thermal conductivity and latent heat for thermal management: Organic PCMs have low thermal conductivity but high latent heat, whereas salt and metallic PCMs have high thermal conductivity but low latent heat. While most current PCM composite literature experiment with only one phase changing material, ours evaluates a composite with two phase change materials. Our inorganic material is Fields Metal (a eutectic alloy of Bi, In, and Sn) and our organic material is paraffin wax. Common variables for thermal management indication, such as a figure of merit for the cooling capacity η_{eff}, energy density E_{eff}, and the thermal conductivity k_{eff}, were found to be larger when our Field's Metal, Paraffin composite PCM was paired with other high latent heat metals, such as Aluminum (Al), Graphitic Carbon Fiber (GCF), and Copper (Cu). The thermal conductivity of our PCM, was compared with other well known numerical PCM models using COMSOL simulations, and found to follow most closely with a parallel model. The parallel model was then used to define equations to calculate the optimal volume fraction of Al, GCF, Copper, for varying volume fractions of Fields metal. Results show that optimal eff values occur at around a 50% volume fraction of metal and 50% volume fraction of PCM, where 50% of the PCM is field's metal (something on timescale result). Additionally, Al, GCF and Cu showed around a 70% increase in cooling capacity and around a 220% increase in energy density when paired with Field's Metal. These results prove to be significant in the understanding of how a composite PCM, where both organic and metallic components change phase, can be beneficial to various applications in thermal management. [1] [2] [3] [4] [5]

I. INTRODUCTION

Phase Changing Materials have wide variety of current applications in the modern day such as in solar power plants, solar heating and cooling systems, heat recovery systems, photovoltaic electricity systems, space industry, and thermal management of high power electronic equipment: where PCMs are designed to change phase and absorb latent heat at peak energy loads during operation, then dissipating this energy at a later time to prevent overheating. The research in this paper deals with a composite PCM consisting of Field's Metal and Paraffin wax. Paraffin wax has an exceptional specific latent heat capacity of $24.35\frac{KJ}{kg}$, while Field's Metal has a decent thermal conductivity of $18.75\frac{W}{mK}$ in addition to it's

high volumetric latent heat capacity of $188.469\frac{MJ}{kg}$. When put together, these material characteristics benefit each other resulting in an optimized PCM. Furthermore the additions of other commonly used non PCM metals with high thermal conductivity's, such as Aluminum (Al) $205\frac{W}{mK}$, Graphitized Carbon Fiber (GCF) $600\frac{W}{mK}$, and Copper (Cu) $385\frac{W}{mK}$, increases the speed at which heat can be absorbed from the environment in varying applications [1]. Figures of merit and material characteristics serve as essential indicators for a materials thermal management ability and application in the real world. The following study deals with the cooling capabilities of a composite PCM and its incorporation with Al, GCF, and Cu.

II. THEORY

A. STEFAN PROBLEM

The Stefan problem, or Stefan-Neumann problem (for two region melting), describes the scientific phenomena that occurs during a materials change of phase when solidifying or melting. As such, it is an important process to describe when dealing with phase changing materials. The following boundary and initial conditions must be made to describe the Stefan-Neumann problem.

1) Boundary and Initial Conditions

1) The PCM is modelled as a semi-infinite material
2) An initial temperature T_i is applied to the PCM. T_i is lower than the melting temperature T_m in melting or higher in solidification
3) On one face of the material a wall temperature T_0 is applied
4) Other surfaces are adiabatic and completely insulated
5) A moving boundary s(t) defines the solid liquid interface within the PCM

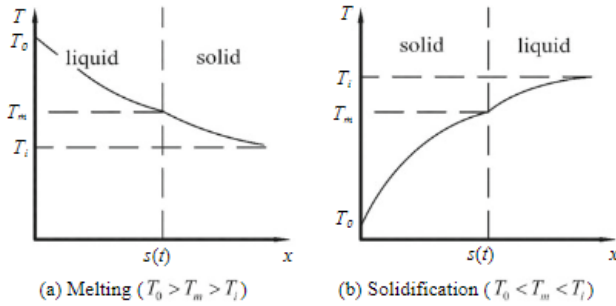Seen below in Fig. 1 is a 2 dimensional representation of a PCM when it is changing phases.

FIGURE 1. 2D representation of the two region melting and solidification in Stefan-Neumann problem [1].

Solving for the temperature distribution at any given location and time withing these two regions is the aim of solving the Stefan problem. This can be done with a close examination of the governing equations.

B. GOVERNING EQUATIONS

Equations seen in Fig. 2 are the fundamental building blocks in understanding the analytical solution to the Stefan problem. Here, some new dimensionless variables are defined in order to simplify the problem. $\theta(X,\tau)$ represents the temperature distribution within the two regions and Ste stands for the Stefan number.

Upon further simplification and the introduction of the variable λ, in Eq. 1

$$\lambda = Ste/2\tau^{1/2} \tag{1}$$

Eq. 2 can be obtained to solve for λ

$$0=\frac{T_m-T}{T_m-T_0} \quad \theta_i=\frac{T_m-T_i}{T_m-T_0} \quad X=\frac{x}{L} \quad S=\frac{s}{L} \quad \tau=\frac{\alpha_1 t}{L^2} \\ N_\alpha=\frac{\alpha_2}{\alpha_1} \quad N_k=\frac{k_2}{k_1} \quad Ste=\frac{c_{p_1}(T_m-T_0)}{h_{sl}} \tag{5.34}$$

where L in Eq. (5.34) is a characteristic length of the problem and can be determined by the nature of the problem or requirement of the solution procedure. The dimensionless governing equations are as follows:

$$\frac{\partial^2\theta_1}{\partial X^2}=\frac{\partial\theta_1}{\partial\tau}, \qquad 0<X<S(\tau), \quad \tau>0 \tag{5.35}$$

$$\theta_1(X,\tau)=1, \qquad X=0, \quad \tau>0 \tag{5.36}$$

$$\frac{\partial^2\theta_2}{\partial X^2}=\frac{1}{N_\alpha}\frac{\partial\theta_2}{\partial\tau}, \qquad S(\tau)<X<\infty, \quad \tau>0 \tag{5.37}$$

$$\theta_2(X,\tau)\to\theta_i, \qquad X\to\infty, \quad \tau>0 \tag{5.38}$$

$$\theta_2(X,\tau)=\theta_i, \qquad X>0, \quad \tau=0 \tag{5.39}$$

$$\theta_1(X,\tau)=\theta_2(X,\tau)=0, \qquad X=S(\tau), \quad \tau>0 \tag{5.40}$$

$$-\frac{\partial\theta_1}{\partial X}+N_k\frac{\partial\theta_2}{\partial X}=\frac{1}{Ste}\frac{dS}{d\tau}, \qquad X=S(\tau), \quad \tau>0 \tag{5.41}$$

FIGURE 2. Stefan-Neumann governing equations [1].

$$\frac{e^{-\lambda^2}}{erf(\lambda)}+\frac{N_k*\theta_i*e^{\frac{-\lambda^2}{N_\alpha}}}{N_\alpha^{1/2}*erfc(\lambda/N_\alpha^{0.5})}=\frac{\lambda*\sqrt{\pi}}{Ste} \tag{2}$$

Once λ is obtained, it can be used to solve for the temperature distributions θ_1 and θ_2, seen in Eq.3 and Eq.4 where the subscripts 1 and 2 stand for the solid and liquid regions of the melting PCM.

$$\theta_1(X,\tau)=1-\frac{erf[X/2\tau^{1/2}]}{erf(\lambda)} \tag{3}$$

$$\theta_2(X,\tau)=1-\frac{erfc[X/2(N_\alpha*\tau)^{1/2}]}{erfc(\frac{\lambda}{(N_\alpha)^{(1/2)}})} \tag{4}$$

In addition to the temperature distribution, the heat flux across one end (wall) of a PCM q'' can be solved, if that wall has a constant temperature boundary condition [2].

$$q''(0,t)=\frac{T_w-T_m}{\sqrt{\pi}\sqrt{t}}*\frac{1}{erf\lambda}*\frac{k_1}{\sqrt{\alpha_1}} \tag{5}$$

Where $q''(0,t)$ is heat flux per unit area, T_w is wall temperature, T_m is melting point, t is time in seconds, and k_1 and α_1 are the thermal conductivity and thermal diffusivity of the liquid region in the PCM.

The cooling capacity figure of merit η, used for material optimization in this paper's study, can be derived from Eq.5. η represents a measure of a PCM's ability to absorb heat [4]. This figure of merit will be described with more detail in section IV.

III. SIMULATIONS FOR VALIDATION

When dealing with composite PCMs, it is always advantageous to assume the materials within the PCM are homogeneously assorted, since it allows for simplicity when calculating effective material characteristics. Our group used COMSOL Multiphysics to further investigate the thermal response of our Field's Metal and Paraffin composite PCM. A 0.1mm by 0.1mm by 1mm rectangular column was used to represent our PCM at varying volume fractions of Paraffin,

seen in Fig. 3. The spheres represent the Paraffin and the rest represents the Field's metal.
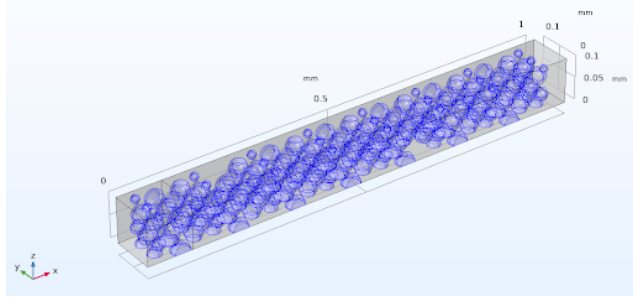

FIGURE 3. 3D view of Paraffin (spheres) and Field's Metal (rectangular block) composite in COMSOL

A fixed temperature was applied to one end, while the opposite end was considered adiabatic. The other four faces had periodic boundary conditions applied.

The heat transfer response of our PCM was numerically analyzed through COMSOL's Finite Element Model (FEM) and compared with well known theoretical models of material characterization, to be matched with a model of best fit. Fig. 4 shows that for 21.8% 40.3% and 50.1% volume fractions of Paraffin, the thermal conductivity k calculated through COMSOL most closely fit a parallel model.
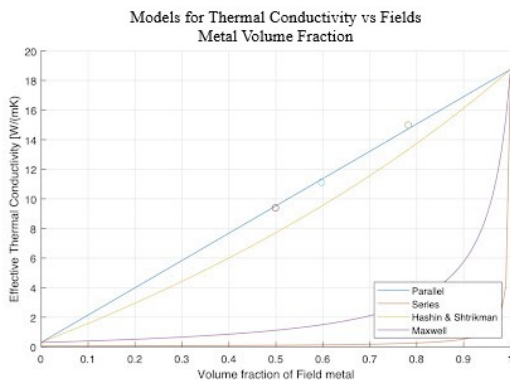

FIGURE 4. COMSOL simulation showing that it most closely follows the parallel model in composite based solutions.

As a result of this finding, equations used in our analysis assumed that composite materials were in parallel with each other.

IV. ANALYSIS

A. VARIABLES FOR MATERIAL ANALYSIS

The most significant variable used in analysis was η a figure of merit derived through the discovery that the heat flux in Eq. (5) mainly depends on two variables: thermal conductivity and volumetric latent heat. [1]

$$\eta = \sqrt{k_{eff} * L_v}. \tag{6}$$

Where k_{eff} is the effective thermal conductivity [W/mK] and L_v is the volumetric latent heat [J/kg]. Together they represent the two variables a materials cooling capability most heavily relies on.

The second variable used in our analysis, is effective energy density E_{eff} [J/kg]. The effective energy density shown in Eq.7, is essentially a weighted average, using a parallel model, of latent and sensible heat among the materials in a composite, and is crucial to understanding a materials thermal storage capabilities.

$$E_{eff} = (C_{v,FM} * \Delta T + L_{v,FM})\phi + (C_{v,P} * \Delta T + L_{v,P})(1 - \phi). \tag{7}$$

C_v [J/kg*K], is a materials specific heat capacity when absorbing sensible heat, and because during this phase change process $C_v << L_v$, Eq.7 can be further simplified to Eq.8

$$E_{eff} = (H_{v,FM})\phi + (H_{v,P})(1 - \phi) \tag{8}$$

Finally, the thermal conductivity k is approximated, again using the parallel method, and shown in Eq.9.

$$k_{eff} = (k_{FM})\phi + (k_P)(1 - \phi) \tag{9}$$

B. TESTING SETUP

These equations were used in MATLAB to plot the cooling capacity figure of merit for various metals combined with PCM (see supplementary information S.2). Graphitized Carbon Fiber, Aluminum, and Copper were modeled at varying volume fractions with and without a Field's Metal PCM over a 10 Kelvin temperature range, where the PCM (which has a lower melting point) melts, and the other metal does not and purely absorbs sensible heat. While the volume fractions of the metals were varying from 0-100%, three scenarios were modeled: When the volume fraction of Field's metal inside the (Paraffin + Field's Metal PCM) was 0.25, 0.5, and 0.75. This allows for an analysis to see which volume fraction of non melting metal(Al, GCF, Cu), Field's Metal, and Paraffin wax, leads to an optimal figure of merit. Graphs for the Figure of Merit vs. Effective Energy Density were also plotted to analyze their dependencies.

V. RESULTS AND DISCUSSION

A. COOLING CAPACITY FIGURE OF MERIT

Fig.5 (a,b,c), showing the results of the figure of merit, led to significant results. Notably, Al, GCF, and Cu, had a larger cooling capacity when Field's Metal was included. This increase in cooling capacity was most apparent at a 50% volume fraction of Field's Metal inside the PCM: Aluminum (Al), Graphitized Carbon Fiber (GCF), and Copper (Cu) exhibited a 72% ,72%, and 67% increase respectively. This increase is due to Field's Metal's significant contribution to the thermal conductivity and specific latent heat of the PCM composite. The largest cooling capacity of the three material composites was Graphitized Carbon Fiber at $2.34 * 10^5 [W s^{0.5} K^{-1} m^{-2}]$, due to it having the largest thermal conductivity k. Additionally, the straight line, representing pure PCM (Paraffin and Field's Metal) yielded a lower cooling coefficient than when a second non melting metal was added. These results specifically, further support the need for the addition of Field's Metal to create a PCM composite when dealing with high thermal conductivity metal such as Aluminum, Graphitized Carbon Fiber, and Copper, in thermal management applications.

Furthermore, all graphs in Fig.5 peak around a middle range of metal volume fraction, that is because effective thermal conductivity increases with the volume fraction of metal, while the effective energy density decreases, leading to a peak values that correspond to mid range volume fractions when using Eq.5. Peak figure of merits for all material combinations occur within a 0.49-0.61 (49-61%) volume fraction of Aluminum, Graphitized Carbon Fiber, or Copper. Additionally, 0.5 (50%) volume fractions of Field's Metal inside the PCM provide the highest figures of merit. This provides a nice constraint for the ratio of materials and further validates the cooling advantage of composite PCMs: Both too much and too little metal decrease the figure of merit, finding the right amount is optimal in material design.

When analyzing Fig.6 it is important to note that, unlike Fig 5 the volume fraction of metal is changing now from 0-100% from right to left (in the opposite direction), additionally the same code was used seen in S.2 of supplementary information. Fig 6 shows the figure of merit plotted against the effective energy density of the six PCM, metal combinations. When optimizing these materials, ideally the largest effective energy density would correspond to the largest cooling capacity figure of merit, however this is not what graph trends show. The figure of merit steadily increases with the effective energy density before it suddenly drops at higher densities. This is because the volume fraction of Al, GCF, and Cu are now 0, minimizing the thermal conductivity, and in turn minimizing the figure of merit η. Supplementary information S.1 shows the energy density that corresponds to the largest figure of merit. Energy density values are shown to be largest around a 50% volume fraction of Field's Meal in PCM, but further research should be made to discover which specific volume fraction of Field's Metal yields the largest values. Regardless, with the addition 50% Field's Metal in the PCM, Aluminum (Al), Graphitized Carbon Fiber (GCF), and Copper (Cu) exhibited a 226% , 217%, and 220% increase in maximum energy density, respectively. Finally, the maximum figure of merit η, in Fig. 6, occurs not too far away from the maximum effective energy density E_{eff}. So when choosing a material combination that has a large figure of merit and energy density, not much sacrifice has to be made to find a middle ground between these two material characteristics.
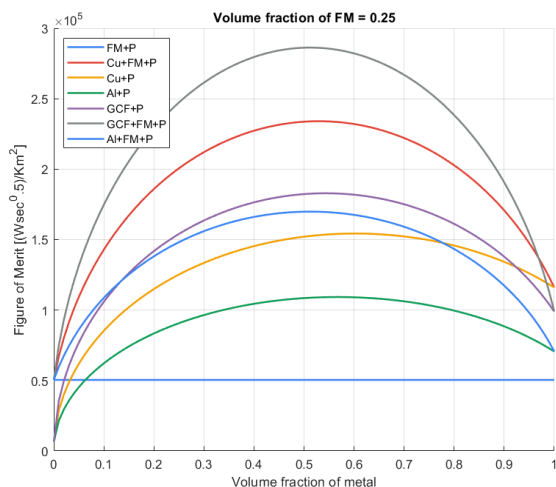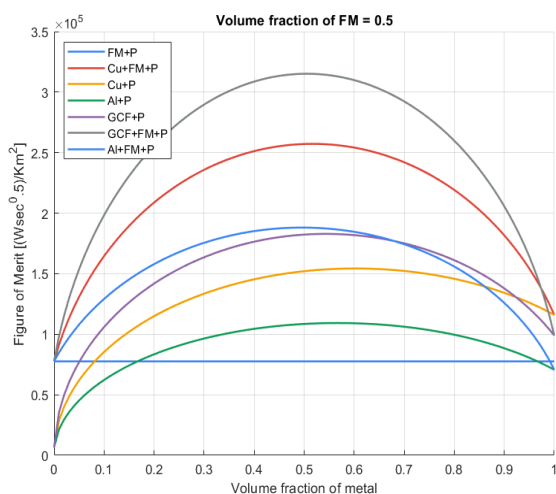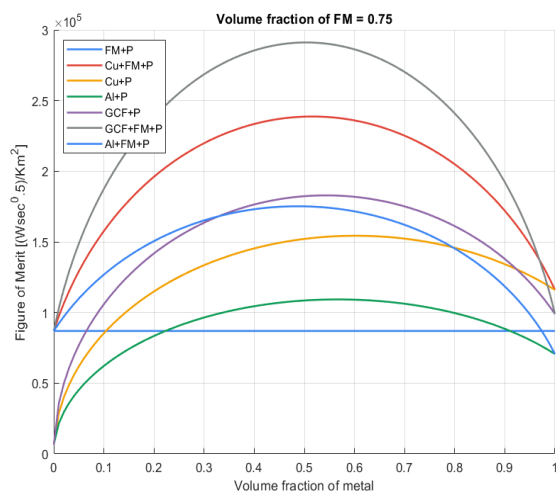
FIGURE 5. Figure of Merit vs Al, GCF, and Cu volume fractions at varying Field's Metal volume fractions in the PCM

FIGURE 6. Figure of Merit vs Effective Energy Density for varying volume fractions of Field's Metal in the PCM

VI. CONCLUSION

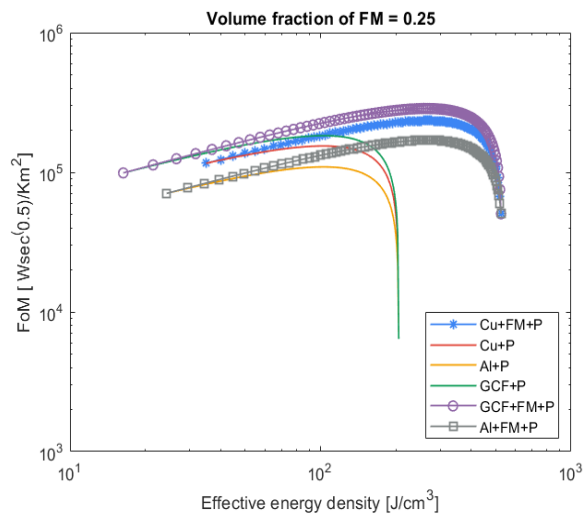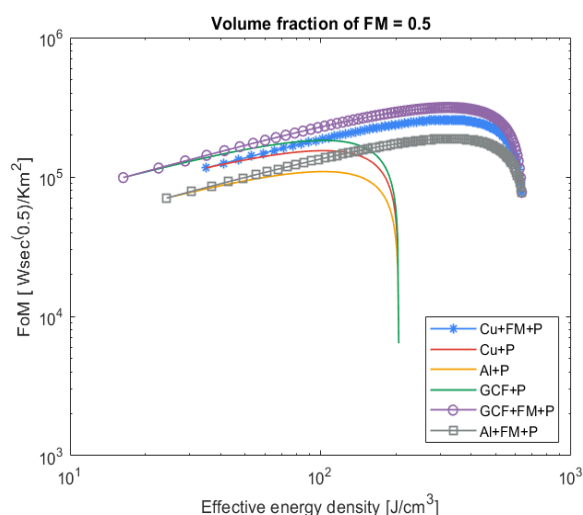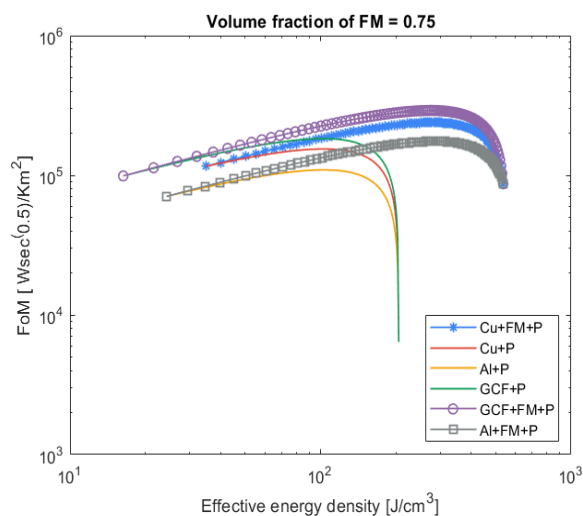Phase changing materials are known to have exceptional heat storage capabilities, with a wide range of applications. Recently, many studies have been released on composite materials which incorporate an organic PCM such as paraffin wax, with a high specific latent heat capacity for energy storage during phase change, and a non PCM metal with a high thermal conductivity. Our study expands upon this with the use of a metallic PCM, Field's Metal, in addition to the organic PCM, Paraffin, to increase the volumetric latent heat capacity which Paraffin lacks. Results show that, at 50% Field's Metal inside the PCM, Aluminum (Al), Graphitized Carbon Fiber (GCF), and Copper (Cu) exhibited a 72% ,72%, and 67% increase in it's cool capacity η and 226% , 217%, and 220% increase in maximum energy density, respectively.

With such a significant increase in the cooling capacity and energy density, composite PCM's paired with high conductivity metals look to have a bright future for application in the world of thermal management. The addition of non-melting metals such as Aluminum, Graphitized Carbon Fiber, and Copper, allow for a rigid solid boundary between the PCM and its heat transfer application, if the PCM was to hypothetically be placed inside the metal. A follow up paper is soon expected, and will focus on the development and experimentation of the composite PCM and metals focused on in this paper. Results will then be compared with literature and simulation to provide a more holistic report.

.

APPENDIX A SUPPLEMENTARY MATERIAL

S.1

```
6     %% Given Data:
7
8     del_T = 10;
9     Phi = linspace(0,1);                  % Volume fraction of metal
10    Phif = 0.25;                          % Volume fraction of fields metal
11
12    % Fields metal:
13
14    k_f = 18.75;                          % Thermal conductivity of fields metal in W/mK
15    h_f = 25400;                          % Latent Heat of fields metal in J/kg
16    rho_f = 7880;                         % Density of fields metal in Kg/m^3
17    cp_f = 325;                           % Specific heat capacity of fields metal in J/KgK
18    Cp_f = cp_f*rho_f;                    % Specific heat capacity of fields metal in J/m^3K
19    H_f = h_f*rho_f;                      % Latent heat of fields metal in J/m^3
20
21    % Paraffin:
22
23    k_p = 0.2;                            % Thermal conductivity of paraffin in W/mK
24    h_p = 243500;                         % Latent Heat of paraffin in J/kg
25    rho_p = 774;                          % Density of paraffin in Kg/m^3
26    cp_p = 2160;                          % Specific heat capacity of paraffin in J/KgK
27    Cp_p = cp_p*rho_p;                    % Specific heat capacity of paraffin in J/m^3K
28    H_p = h_p*rho_p;                      % Latent heat of paraffin in J/m^3
29
30    % Cu:
31
32    k_Cu = 385;                           % Thermal conductivity of copper in W/mK
33    rho_Cu = 8960;                        % Density of copper in Kg/m^3
34    cp_Cu= 390;                           % Specific heat capacity of copper in J/KgK
35    Cp_Cu = cp_Cu*rho_Cu;                 % Specific heat capacity of copper in J/m^3K
36

37    %Al:
38
39    k_Al = 205;                           % Thermal conductivity of Aluminum in W/mK
40    rho_Al = 2700;                        % Density of Aluminum in kg/m^3
41    cp_Al = 900;                          % Specific heat capacity of Aluminum in J/kgK
42    Cp_Al = cp_Al*rho_Al;                 % Specific heat capacity of Aluminum in J/m^3K
43
44    % GCF:
45
46    k_GCF = 600;                          % Thermal conductivity of copper in W/mK
47    rho_GCF = 2266;                       % Density of copper in Kg/m^3
48    cp_GCF = 720;                         % Specific heat capacity of GCF in J/kgK
49    Cp_GCF = cp_GCF*rho_GCF;              % Specific heat capacity of GCF in J/m^3K
50
51    %Paraffin + Fields metal:
52
53    h_pcm = h_f.*Phif + (h_p.*(1-Phif));  % Effective Latent heat of pcm in J/kg
54    cp_pcm = cp_f.*Phif + (cp_p.*(1-Phif)); % Effective Specific heat capacity of pcm in J/kgK
55    rho_pcm = rho_f.*Phif + (rho_p.*(1-Phif)); % Effective density of pcm in Kg/m^3
56    H_pcm = h_pcm.*rho_pcm;               % Effective Latent heat of pcm in J/m^3
57    Cp_pcm = cp_pcm.*rho_pcm;             % Effective Specific heat capacity in J/m^3K

61    % Thermal conductivity:
62    k1 = k_f.*Phif + (k_p.*(1-Phif));     % Effective Thermal conductivity of pcm in W/mK
63    k2 = k_Cu.*Phi + (k1.*(1-Phi));       % Effective Thermal conductivity of Cu+pcm in W/mK
64    k3 = k_Cu.*Phi + (k_p.*(1-Phi));      % Effective Thermal conductivity of Cu+paraffin in W/mK
65    k4 = k_Al.*Phi + (k_p.*(1-Phi));      % Effective Thermal conductivity of Al+paraffin in W/mK
66    k5 = k_GCF.*Phi + (k_p.*(1-Phi));     % Effective Thermal conductivity of GCF+paraffin in W/mK
67    k6 = k_GCF.*Phi + (k1.*(1-Phi));      % Effective Thermal conductivity of GCF+pcm in W/mK
68    k7 = k_Al.*Phi + (k1.*(1-Phi));       % Effective Thermal conductivity of Al+pcm in W/mK
69
70    % Energy density:
71    E_eff_1 = Phi*0 + ((H_pcm + (Cp_pcm*del_T)))*0.000001;        % Effective Energy density of pcm in J/cm^3
72    E_eff_2 = ((((Cp_Cu*del_T)).*Phi) + ((H_pcm + (Cp_pcm*del_T)).*(1-Phi)))*0.000001; % Effective Energy density of Cu+pcm in J/cm^3
73    E_eff_3 = ((((Cp_Cu*del_T)).*Phi) + ((H_p + (Cp_p*del_T)).*(1-Phi)))*0.000001;  % Effective Energy density of Cu+paraffin in J/cm^3
74    E_eff_4 = ((((Cp_Al*del_T)).*Phi) + ((H_p + (Cp_p*del_T)).*(1-Phi)))*0.000001;  % Effective Energy density of Al+paraffin in J/cm^3
75    E_eff_5 = ((((Cp_GCF*del_T)).*Phi) + ((H_p + (Cp_p*del_T)).*(1-Phi)))*0.000001; % Effective Energy density of GCF+paraffin in J/cm^3
76    E_eff_6 = ((((Cp_GCF*del_T)).*Phi) + ((H_pcm + (Cp_pcm*del_T)).*(1-Phi)))*0.000001; % Effective Energy density of GCF+pcm in J/cm^3
77    E_eff_7 = ((((Cp_Al*del_T)).*Phi) + ((H_pcm + (Cp_pcm*del_T)).*(1-Phi)))*0.000001;  % Effective Energy density of Al+pcm in J/cm^3
78
79    X1 = times(k1,E_eff_1.0.000001);
80    X2 = times(k2,E_eff_2/0.000001);
81    X3 = times(k3,E_eff_3/0.000001);
82    X4 = times(k4,E_eff_4/0.000001);
83    X5 = times(k5,E_eff_5/0.000001);
84    X6 = times(k6,E_eff_6/0.000001);
85    X7 = times(k7,E_eff_7/0.000001);
86
87    Eta_eff1 = sqrt(X1);                  % Figure of merit of pcm in (Wsec^0.5)/Km^2
88    Eta_eff2 = sqrt(X2);                  % Figure of merit of Cu+pcm in (Wsec^0.5)/Km^2
89    Eta_eff3 = sqrt(X3);                  % Figure of merit of Cu+paraffin in (Wsec^0.5)/Km^2
90    Eta_eff4 = sqrt(X4);                  % Figure of merit of Al+paraffin in (Wsec^0.5)/Km^2
91    Eta_eff5 = sqrt(X5);                  % Figure of merit of GCF+paraffin in (Wsec^0.5)/Km^2
92    Eta_eff6 = sqrt(X6);                  % Figure of merit of GCF+pcm in (Wsec^0.5)/Km^2
93    Eta_eff7 = sqrt(X7);                  % Figure of merit of Al+pcm in (Wsec^0.5)/Km^2
```

FIGURE 7. MATLAB code setup for results

S.2

Volume Fraction of Fields Metal in PCM = 0.25		
Material	η_{max} [W*sec$^{0.5}$*K^{-1}*m^{-2}]	Effective Energy Density [J/cm^3]	Volume Fraction of Metal Φ
Cu+PCM	2.34E+05	268	0.53
Cu+Paraffin	1.54E+05	102	0.61
Al+Paraffin	1.09E+05	103	0.57
GCF+Paraffin	1.83E+05	102	0.55
GCF+PCM	2.86E+05	263	0.52
Al+PCM	1.70E+05	267	0.52

Volume Fraction of Fields Metal in PCM = 0.5		
Material	η_{max} [W*sec$^{0.5}$*K^{-1}*m^{-2}]	Effective Energy Density [J/cm^3]	Volume Fraction of Metal Φ
Cu+PCM	2.57E+05	326	0.52
Cu+Paraffin	1.54E+05	102	0.61
Al+Paraffin	1.09E+05	103	0.57
GCF+Paraffin	1.83E+05	102	0.55
GCF+PCM	3.15E+05	323	0.51
Al+PCM	1.88E+05	333	0.5

Volume Fraction of Fields Metal in PCM = 0.75		
Material	η_{max} [W*sec$^{0.5}$*K^{-1}*m^{-2}]	Effective Energy Density [J/cm^3]	Volume Fraction of Metal Φ
Cu+PCM	2.39E+05	278	0.52
Cu+Paraffin	1.54E+05	102	0.61
Al+Paraffin	1.09E+05	103	0.57
GCF+Paraffin	1.83E+05	102	0.55
GCF+PCM	2.91E+05	273	0.51
Al+PCM	1.75E+05	288	0.49

FIGURE 8. Maximum cooling coefficient figure of merit and corresponding effective energy density and volume fraction of metal (based on data in figures a, b, and c)

ACKNOWLEDGMENT

REFERENCES

[1] T. S. F. Patrick J. Shamberger, "Cooling power and characteristic times of composite heat sinks and insulants."

[2] Y. Z. Amir Faghri, Fundamentals of Multiphase Heat Transfer and Flow. Springer, 2006. [Online]. Available: https://link.springer.com/book/10.1007/978-3-030-22137-9

[3] P. B. W. B. K. P. V. B. N. M. Tianyu Yang, Jin Gu Kang and W. P. King, "A composite phase change material thermal buffer based on porous metal foam and low-melting-temperature metal alloy," Applied Physics Letters, vol. 116, pp. 1–5, 2020.

[4] J. S. K. e. a. Michael T. Barako, Srilakshmi Lingamneni, "Optimizing the design of composite phasechange materials for high thermal power density."

[5] M. McCann, "Expanding the palette: Synthesizing microencapsulated organic phase change materials in metallic matricesfor transient thermal applications," Master's thesis, Washington University in St. Louis, St. Louis MO, 2019.